

Modeling and Position Control of Human Lower Limb Rehabilitation Robot using Pneumatic Muscle Actuators

Mohammed Y. Hassan*(Assist.Prof.) Ph.D Shahad S. Ghintab*

Abstract

The aim of human lower limb rehabilitation robot is to regain the ability of motion and to strengthen the weak muscles. This paper proposes the design and modelling of four Degree Of Freedom (4-DOF) lower limb wearable rehabilitation robot. This robot is located in, hip, knee and ankle joints to enable the patient for motion and turn in both directions. The joints are actuated by Pneumatic Muscles Actuators (PMAs). The PMAs have very great potential in medical applications because the similarity to biological muscles. This work proposes the structure of the robot to eliminate the singularity problem that exists in the inertia matrix. Also, the effects of disturbance on the robot joints and frictions in robot joints and in PMAs are taken into consideration. The designed robot can be used for the right side leg of an elderly persons whose ages beyond 40th years old. Since the 4-DOF rehabilitation robot actuated by PMAs has high nonlinearity. An intelligent position controller to control each joint position is designed and simulated using two schemes; Mamdani PD-like fuzzy logic and Takagi-Sugeno-Kang (TSK)-PD-like Fuzzy logic to improve the time response specifications such as minimum overshoot, minimization of oscillation and disturbance rejection to track the desired medical trajectory. A comparison between the two schemes shows an enhancement in the results of the second type as compared with the first one.

Keywords: Position control, Rehabilitation robot, Pneumatic Muscle Actuators (PMAs), Fuzzy controller.

*University of Technology

List of Symbols

A_i	Homogenous transformation matrix of frame i .
a_i	Distance along X_i (m)
b	PAM thread length (m)
B_f	Viscous friction coefficient in (N.m)
$C(q, \dot{q})$	Coriolis matrix
$D(q)$	Inertia matrix
d_i	Distance along z_{i-1} (m)
F	friction force (N.M)
F_s	Static friction in (N.m)
F_C	Coulomb friction in (N.m)
$G(q)$	gravitational vector torques
$k_{p_i}, k_{v_i}, k_{o_i}$	Proportional, velocity and output gains
L	PMA length (m)
n	Number of turns of the thread
o_i	End effector frame
P	pressure (Kpa)
P_{atm}	Atmosphere pressure (Kpa)
q	Joint angle of link i (rad)
\dot{q}	Velocity (rad/sec)
\ddot{q}	Acceleration (rad/sec ²)
T	Input torque
τ_{di}	External disturbance (N.m)
$u(t)$	Control law
V_s	(Stribeck velocity) (rad/sec)
X, Y_i, Z_i	Axes frame of each joint (m)
α	Angle between joint frames
θ_i	Joint angle of link i (degree)
σ_0	Stiffness coefficient (N.m.s/rad)
σ_1	Damping coefficient (N.m.s/rad)
σ_2	Coefficient of viscous friction (N.m.s/rad).
ΔL_{Max}	Maximum contraction of the length of muscle (m)
ϕ_{Max}	The maximum range of motion (degree)
x_s	Stribeck speed in (rad/sec)
δ_s	Stribeck exponent.

List of Abbreviations

DOF	Degree Of Freedom
DH	Denevit and Hartenberg
FLC	Fuzzy Logic Controller
NB	Negative Big
NM	Negative Medium
NS	Negative Small
PID	Proportional-Integral-Derivative
PS	Positive Small
PM	Positive Medium
PB	Positive Big
PMAAs	Pneumatic Muscles Actuators
PD	Proportional-Derivative
ROM	Range Of Motion
TSK	Takagi-Sugeno-Kang
Z	Zero

1. Introduction

Damage the central nervous system or spinal cord injuries may result in such a loss of upper or lower limb motor functions ^{1}. The process of strengthening muscles to their normal values is a costly lab or requires time and patience. This process is named rehabilitation; the restoration of a person to an optimal level of physical, mental, and social function and well-being. Physical rehabilitation, in a general sense, aims to maintain, restore and develop the human body movements through physical therapy ^{2}. The human lower limb consists of three joints hip, knee and ankle joint as shown in Figure (1) ^{1}. One of the most common disabilities resulted from stroke is Hemi paresis (One-sided paralysis) right side, where the opposite side (left side) of the brain is damaged by stroke and may affect the face, an arm, a leg, or the entire side of the body ^{2}. According to the medical fact, the right leg is amenability to paraplegia more than left leg so this work design rehabilitation robot for right leg.

In recent years, the research on rehabilitation robot has become an important topic. There are several researches deal with this field such as Ollinger. et al. in (2007) that propose 1-DOF for knee joint actuated by electric motor controlled by Proportional-Integral-Derivative (PID) controller

^{3}. Moreover, this work is extended in (2010) to propose a 1-DOF for knee joint actuated by electric motor that uses Inertia compensation emulated by adding a feedback loop. It consists of a low-pass filter acceleration multiplied by a negative gain ^{4}.



Figure (1): Anatomical of Human Lower Limb ^{1}.

Furthermore, Tu Diep and Tran in (2008) introduced a 1-DOF for knee joint actuated by PMA controlled by PID with neural network ^{5}. Akdoğan et al. in (2009) suggested an intelligent controller structure for a knee rehabilitation robot manipulator with 1-DOF. The controller of the robot manipulator works based on impedance control ^{6}. Also, Aminiazar et al. in (2013) proposes 2-DOF for knee and ankle joints controlled by PD controller ^{7}.

It can be noticed from the previous work that they deal with one or two joints of human lower limb through the design. This causes retraction in workspace and reduces the flexibility when interact with human motion. Furthermore, the robots were actuated by electric motors due to their simplicity of modeling control. Friction in the robot joint, either in the

actuators or in the joints mechanism and the effect of disturbances was not taken into consideration in most of the previous works.

In this work, the design a 4-DOF lower limb wearable rehabilitation robot is proposed; it consists of 2-DOF for hip joint, 1-DOF for knee joint and 1-DOF for ankle joint. The proposed robot is designed for the right side leg and its structure can be used for elderly people whose ages are beyond 40th years old, the reason of choose this age group because this age group is more prone to stroke based on statistical studies ^{1}. The PMA actuator has been adapted in this work. It has many advantages such as low cost, clean, safety, lightweight and like biological muscle. The problem of singularity in inertia matrix is solved through adding an extra link. The effects of friction and disturbances acting on the robot joint are added to the simulation and the friction of PMA is also taken into consideration. Comparison between two schemes of PD-like Fuzzy logic controllers (Mamdani and TSK) is made to control each one of the robot joints in order to achieve the desired performances, such as minimum overshoot, minimum oscillation and disturbance rejection during tracking the medical trajectory.

2. The Structure of Proposed Lower Limb Rehabilitation Robot

The front view and side view of proposed structure are shown in Figure (2). Moreover, The frame assignments for a single right side leg of the proposed lower limb 4-DOF rehabilitation robot are defined and depicted in Figure (3).

According to the free body diagram shown in Figure (3), the robot consists of 4-DOF. The first DOF is for Internal/External Rotation for the hip so that the person wearing the exoskeleton can turn into both directions (left and right). The other DOFs are Flexion/Extension for hip joint, knee joint, and ankle joints. These DOFs are sufficient to rehabilitate the motion of a person's leg. All the joints in this design are revolute joints; Where the Z-axis represents the rotational axis for each joint.

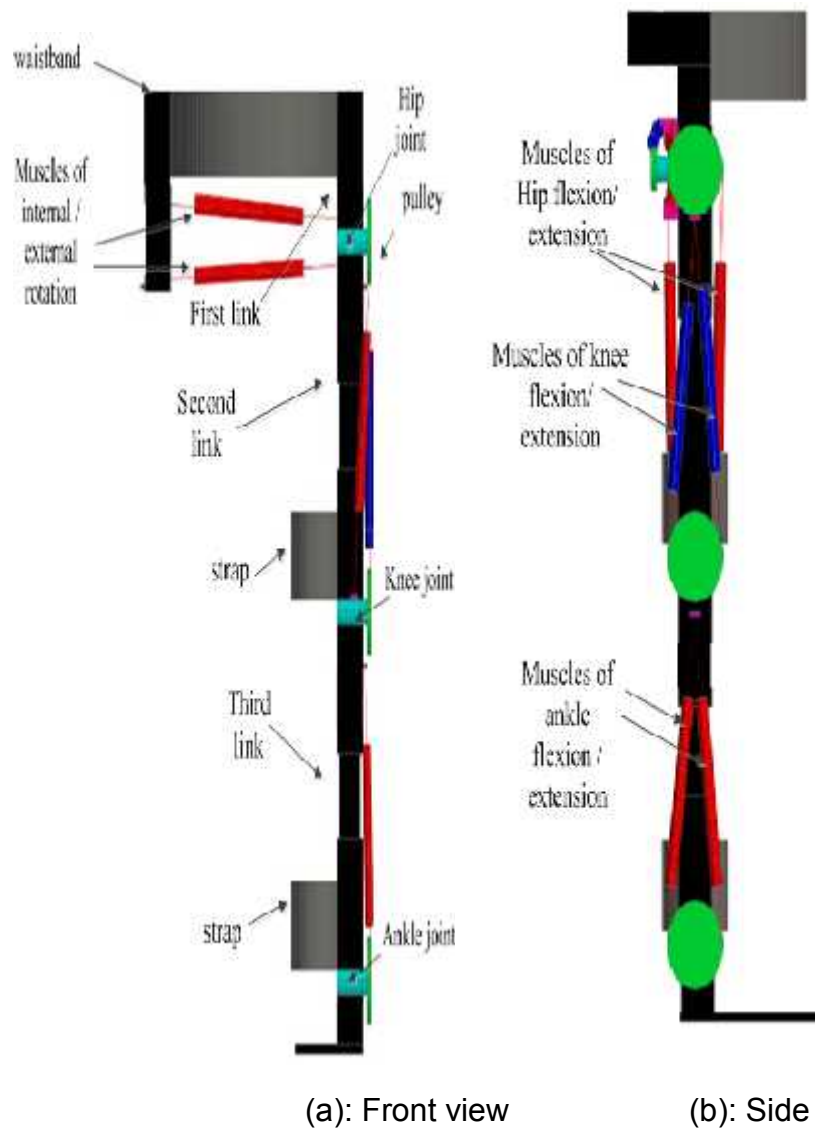


Figure (2): The proposed structure of the wearable rehabilitation robot.

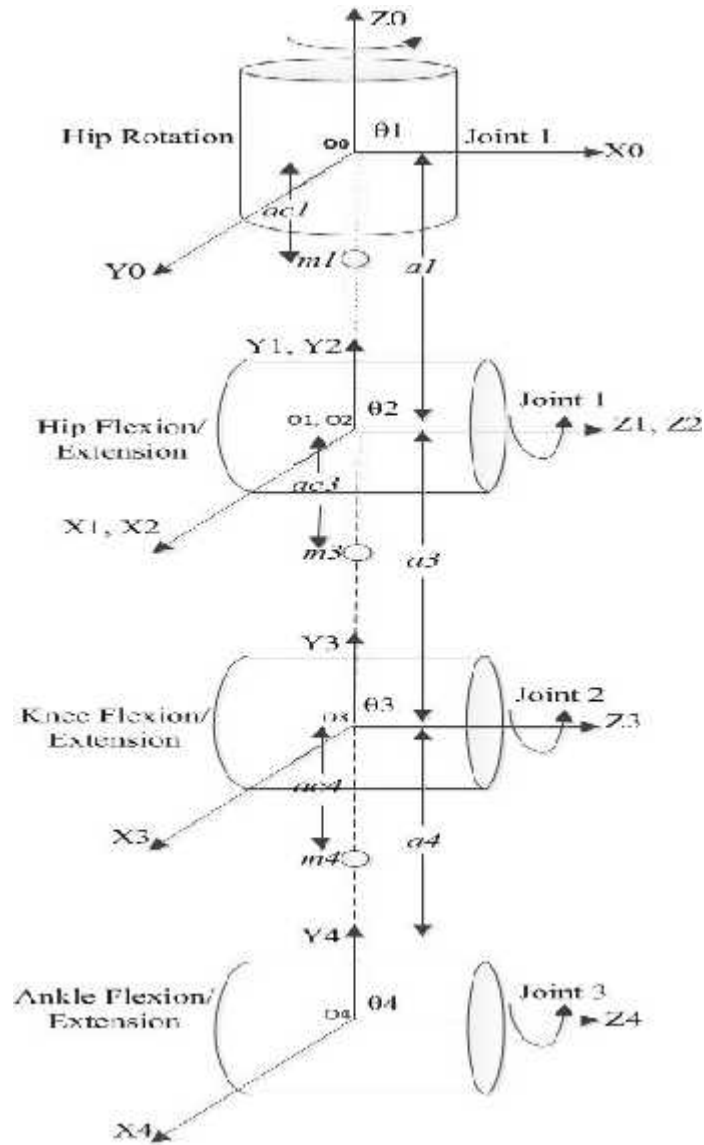


Figure (3): Frame Assignments for a single right side leg of the proposed lower limb Rehabilitation Robot.

2.1 Forward Kinematics:

The first step to design the robot is to define the parameters and set up coordinate systems. The forward kinematics of the proposed rehabilitation robot is performed using **Denevit and Hartenberg method**. Homogeneous transformation matrix (A_i) is^{8}:

$$A_i = \begin{bmatrix} c_{\theta} & -s_{\theta}c_{\alpha} & s_{\theta}s_{\alpha} & a_i c_{\theta} \\ s_{\theta} & c_{\theta}c_{\alpha} & -c_{\theta}s_{\alpha} & a_i s_{\theta} \\ 0 & s_{\alpha} & c_{\alpha} & d_i \\ 0 & 0 & 0 & 1 \end{bmatrix} \dots\dots\dots (1)$$

Where $s_{\theta} = \sin \theta, c_{\theta} = \cos \theta, s_{\alpha} = \sin \alpha$ and $c_{\alpha} = \cos \alpha$. The four quantities θ_i, a_i, d_i , and α_i are parameters associated with link i and joint i , where:

a_i = is the distance along x_i from frame o_i to the intersection of the x_i and z_{i-1} axes.

d_i = is the distance along z_{i-1} from o_{i-1} to the intersection of the x_i and z_{i-1} axes.

α_i = is the angle between z_{i-1} and z_i measured about x_i .

θ_i = is the angle between x_{i-1} and x_i measured about z_{i-1} . θ_i is variable if joint i is revolute. Depending on the above definitions to the parameters and on the frames shown in Figure (3), the DH parameters are listed in Table (1). Thus; the transformation matrix T_0^4 from hip to ankle joint is calculated as:

$$T_0^4 = A_1 \cdot A_2 \cdot A_3 \cdot A_4 = \begin{bmatrix} c_3 c_4 c_{12} - s_3 c_{12} s_4 & -s_4 c_3 c_{12} - c_4 s_3 c_{12} & -s_{12} & a_4 c_4 s_3 c_{12} - a_4 s_4 s_3 c_{12} + a_3 c_3 c_{12} + a_1 c_1 \\ c_3 c_4 s_{12} - s_4 s_3 s_{12} & -s_4 c_3 s_{12} - c_4 s_3 s_{12} & c_{12} & a_4 c_4 c_3 s_{12} - a_4 s_4 c_3 s_{12} + a_3 c_3 s_{12} + a_1 s_1 \\ -s_3 c_4 - c_3 s_4 & s_3 s_4 - c_3 c_4 & 0 & -a_4 s_4 c_3 - a_3 s_3 \\ 0 & 0 & 0 & 1 \end{bmatrix} \dots\dots\dots (2)$$

2.2 Dynamic Analysis:

By using the Euler Lagrange Equation, the general dynamic equation of robotic systems is given in joint space matrix as:

$$D(q)\ddot{q} + C(q, \dot{q})\dot{q} + F\dot{q} + G(q) + \tau_{dis} = T \dots\dots\dots (3)$$

Where: $q \in R^n$ is the $n \times 1$ vector of generalized joint coordinates describing the pose of the manipulator or the joint variable n -vector. $\dot{q} \in R^n$ is the vector of joint velocities. $\ddot{q} \in R^n$ is the vector of joint accelerations $D(q) \in R^{n \times n}$ is the $n \times n$ symmetric joint-space inertia matrix. $C(q, \dot{q}) \in R^{n \times n}$ describes Coriolis and centripetal torques, $F(\dot{q}) \in R^n$ is the friction vector, $G(q) \in R^n$ is the gravitational loading $n \times 1$ vector torques, $\tau_{dis} \in R^n$ represents disturbances which are bounded, and $T \in R^n$ is the joint $n \times 1$ vector of the generalized input torques ⁽⁸⁾

The dynamic equations that describe the proposed 4-DOF lower limb rehabilitation robot are:

$$T_1 = d_{11}\ddot{q}_1 + d_{12}\ddot{q}_2 + d_{13}\ddot{q}_3 + d_{14}\ddot{q}_4 + c_{211}q_2\dot{q}_1 + c_{311}q_3\dot{q}_1 + c_{411}q_4\dot{q}_1 + c_{321}q_3\dot{q}_2 + c_{222}q_2\dot{q}_2 + c_{322}q_3\dot{q}_2 + c_{422}q_4\dot{q}_2 + c_{131}q_1\dot{q}_3 + c_{231}q_2\dot{q}_3 + c_{531}q_3\dot{q}_1 + c_{431}q_4\dot{q}_1 + c_{141}q_1\dot{q}_4 + c_{241}q_2\dot{q}_4 + c_{341}q_3\dot{q}_4 + c_{441}q_4\dot{q}_4 + \emptyset(q_1) + F(\dot{q}_1) + \tau_{ds1} \dots\dots\dots (4)$$

$$T_2 = d_{21}\ddot{q}_1 + d_{22}\ddot{q}_2 + d_{23}\ddot{q}_3 + d_{24}\ddot{q}_4 + c_{112}q_1\dot{q}_2 + c_{312}q_3\dot{q}_2 + c_{412}q_4\dot{q}_2 + c_{322}q_3\dot{q}_2 + c_{422}q_4\dot{q}_2 + c_{132}q_1\dot{q}_3 + c_{232}q_2\dot{q}_3 + c_{142}q_1\dot{q}_4 + c_{242}q_2\dot{q}_4 + \emptyset(q_2) + F(\dot{q}_2) + \tau_{ds2} \dots\dots\dots (5)$$

$$T_3 = d_{31}\ddot{q}_1 + d_{32}\ddot{q}_2 + d_{33}\ddot{q}_3 + d_{34}\ddot{q}_4 + c_{113}q_1\dot{q}_3 + c_{213}q_2\dot{q}_3 + c_{413}q_4\dot{q}_3 + c_{123}q_1\dot{q}_2 + c_{223}q_2\dot{q}_2 + c_{433}q_4\dot{q}_3 + c_{143}q_1\dot{q}_4 + c_{343}q_3\dot{q}_4 + c_{443}q_4\dot{q}_4 + \emptyset(q_3) + F(\dot{q}_3) + \tau_{ds3} \dots\dots\dots (6)$$

$$T_4 = d_{41}\ddot{q}_1 + d_{42}\ddot{q}_2 + d_{43}\ddot{q}_3 + d_{44}\ddot{q}_4 + c_{114}q_1\dot{q}_4 + c_{214}q_2\dot{q}_4 + c_{124}q_1\dot{q}_2 + c_{224}q_2\dot{q}_2 + c_{334}q_3\dot{q}_3 + c_{134}q_1\dot{q}_3 + c_{314}q_3\dot{q}_1 + \emptyset(q_4) + F(\dot{q}_4) + \tau_{dis4} \dots\dots\dots (7)$$

2.3 Joints Friction model:

The nonlinear friction is one of the important factors that affect the motion equation. The

Friction is assumed to be described by the so-called LuGre model. The LuGre model considers friction as a function of the bristle displacement, bristle velocity and the system velocity ⁽⁹⁾:

$$F_{fmodel} = \sigma_0 z + \sigma_1 \dot{z} + f(v) \dots \dots \dots (8)$$

$$\dot{z} = v - \sigma_0 * |v| * z / g(v) \dots \dots \dots (9)$$

Where (z) is the average deflection of the bristles before slipping, (σ_0) is their stiffness coefficient in (N.m.s/rad), (σ_1) is the damping coefficient in (N.n.s/rad) which stabilizes the dynamics in the Stribeck region and (σ_2) is the coefficient of viscous friction in (N.m.s/rad).

The $g(v)$ function models the Stribeck effect as a function of velocity. If (v_s) is the velocity at which Stribeck effect takes place (Stribeck velocity) (rad/sec), then $g(v)$ can be expressed as⁽⁹⁾:

$$g(v) = f_c + (f_s - f_c) * e^{-\frac{v}{v_s}} \dots \dots \dots (10)$$

$$f(v) = \sigma_2 * v \dots \dots \dots (11)$$

v_s is the sliding speed coefficient which determines the stribeck curve and $g(v)$ is such that $f_c \leq g(v) \leq f_s$.

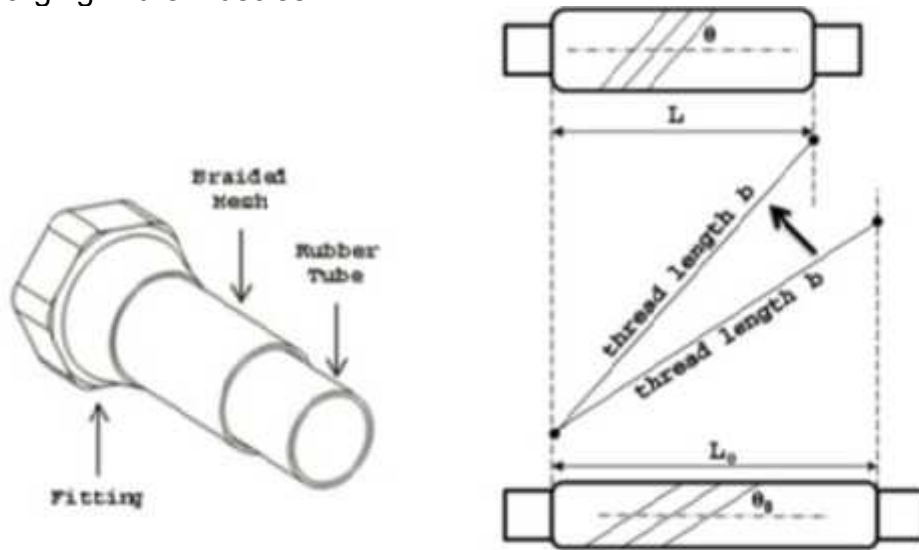
2.4 Solving Singularity problem:

The Jacobian matrix is one of the most important quantities in the analysis and control of robot motion. Previous research works, assumed that the torques of two DOFs at the same joint is the same for simplicity. This causes singularity in (D) inertia matrix related to the singularity in jacobain matrix. In this work, it is assumed that the frame assignment started from pelvis and derived the dynamic model to get torque for each DOF in order to solve this problem. In this case, depending on how the DH parameters have been assigned, a value of (a1= d) is assumed the distance between frame zero and frame one as shown in Figure (3).

3. PMA actuators^{10}:

The PMA is composed of an air-tight tube surrounded by an inextensible braided mesh, a Schematic is given in Figure (4-a). As the internal volume is pressurized, the tube expands radially and shortens in the axial direction, which generates a pulling force in the axial direction. This functioning mechanism is represented by the schematic given in Figure (4-b). This makes the PMA very simple and light-weight device, and gives it a considerable higher power density than other traditional actuators. The amount of force generated by the PMA decreases with the contraction of the muscle, a similar characteristic to that of biological

muscles. Thus, due to the high power density coupled with similar function of biological muscles, the PMA has been utilized frequently in mobile robotics, specifically with humanoid robotics as well as robotic rehabilitation. The reasons of using this type of actuator in this work are because its low mass, excellent power/weight ratio, inherent safety, natural compliance, cleanness and low cost. Pair of PMAs put into antagonism configuration imitate a bicep-tricep system and emphasize the analogy between this muscle actuator and human skeletal muscle. To control exactly the pressure in each muscle, pair of proportional directional control valves is used to control the air mass flow charging and discharging in the muscles.



(a) : Schematic of PMA.

(b): PMA under pressure.

Figure (4): Structure of PMA ^{10}.

When the control signal is changed, the pressure in muscles is changed. As a result, the lengths of the actuators change, (if one muscle shortens, the second one is lengthen approximately the same amount) and the forces exerted makes the robot leg rotate ^{10}.

The force in each muscle is:

$$F_{12} = (P_{12} - P_{atm}) \left\{ \frac{3L^2 - b^2}{4\pi n^2} \right\} \dots \dots \dots (12)$$

The main objective for this design is to match the maximum torque and the range of motion requirements for joints. The design of the lower limb joints consists of cable-pulley mechanism to translate the linear motion of the PMA to a rotary motion. Therefore; in order to provide the proper range of motion and the required torque, the radius of pulley is the most critical design constraint. To properly size the pulley, first the range of motion and torque requirements of the joint are needed. The pair of antagonistic muscle actuators produces the torque (T) in (N.m) on the pulley wheel which can be defined as:

$$T = (F_1 - F_2) \cdot R_{pull} = I \cdot \ddot{\theta} + b \cdot \dot{\theta} + k \cdot \theta + F_{fPMA} \dots\dots\dots (13)$$

Where the radius of the pulley R_{pull} (m) can be calculated by

$$R_{pull} = \frac{\Delta L_{Max}}{\phi_{max}} \dots\dots\dots (14)$$

ΔL_{Max} in (m) is the maximum contraction of the length of muscle and ϕ_{Max} in (degree) is the maximum range of motion. This torque is used as an input to the robot. The PMA friction is presented by the following static model ^{11}:

$$F_{fPMA} = \begin{cases} F(v) & \text{if } \dot{\theta} \neq 0 \\ F_L \dot{\theta} = 0 \text{ and } |F_L| < F_s & \dots\dots\dots (15) \\ F_s \cdot \text{sgn}(F_L) & \text{otherwise } \dot{\theta} = 0 \text{ and } |F_L| > F_s \end{cases}$$

Where $F(v)$ is an arbitrary function and F_s is the static friction in (N.m). The arbitrary function can be represented by a Stribeck nonlinear function as ^{11}:

$$F(v) = F_C + (F_S - F_C) \cdot e^{-\left(\frac{\dot{\theta}}{\alpha \delta_s}\right)^{\delta_s}} + B_f \cdot \dot{\theta} \dots\dots\dots (16)$$

Where F_C is Coulomb friction in (N.m), $\dot{\theta}$ is angular velocity in (rad/sec), $\alpha \delta_s$ is the Stribeck speed in (rad/sec), B_f is the viscous friction coefficient in (N.m) and δ_s is the Stribeck exponent.

4. Simulation of the Proposed Rehabilitation Robot:

The structure of the proposed rehabilitation robot depends on the standard dimensions of human body length and mass for a patient of age beyond 40th years old ^{2}, where ($a_1 = 0.1$ m) represents the length between the

pelvises to the hip joint, and the links ($a_3 = 0.48\text{ m}$) and ($a_4 = 0.44\text{ m}$) are equivalent to the thigh, and calf of human body respectively. Range Of Motion (ROM) of rehabilitation robot must be more than ROM of biological human during walking and less than maximum ROM to make the design of rehabilitation robot more flexible and don't restrict the motion of patient. The selected ROMs of the proposed design are listed in Table (2). Two four-way proportional control valves, (FESTOMPYE-5-M5-010-B), were selected to control the airflow of the PMAs. It can adjust flow-rate according to the input voltage within the range from 0 to 10 V by changing the spool position. Depending on the ROM of the proposed robot and the peak torques for the joints of a human leg listed in Table (3), the radius of pulley can be calculated according to equation (16). Given 10% maximum contraction of the muscle length, where the length of each muscle is 0.5 m, the maximum contraction of the length is 0.05 m and depending on the ROM, the selected radius of pulley for the joints are 0.038 m, 0.038 m, 0.044 m and 0.057 m respectively. The torque calculated by equation (12). The parameters of the PMA and the proportional directional control valves are depicted in Table (4). The disturbances that affect in this biomedical rehabilitation robot are come from the convulsions in the human leg muscles. One of the functions used to represent the disturbances generated from the unexpected shocks and stack to the human leg is the sinusoidal signal. The disturbance is represented in this work by:

$$\tau_{dis} = A * \sin(\omega t) \dots \dots \dots (17)$$

In this work assume the frequency of disturbance is $\omega = 1\text{ rad/sec}$, and amplitude $A = 4\text{ v}$, where this value is sufficient to describe the convulsions for human lower leg.

However, the parameters of the joint friction model and PMA friction model are listed in Table (5), and Table (6).

5. Controller Design:

Since the 4-DOF rehabilitation robot and PMA have high nonlinearity, Fuzzy Logic Controller (FLC) has the ability to deal with this nonlinearity and to achieve tracking performance such as minimum overshoot, minimum oscillation and disturbance rejection. A FLC of Mamdani PD-like Fuzzy type is designed. The inputs of the controller are the (error (e) and rate of error (\dot{e})) Where the control signal is:

$$u(t) = kp_1 e(t) + kv_1 \dot{e}(t) \dots \dots \dots (18)$$

Seven Gaussian shaped membership functions are used for each input and output, see Figure(5). The inputs and output scaling factors are defined as:

(proportional gain (k_p), derivative gain (k_v), and output gain (k_o)). The linguistic variables of the membership functions of the FLC are; NB (Negative Big), NM (Negative Medium), NS (Negative Small), Z (Zero), PS (Positive Small), PM (Positive Medium), and PB (Positive Big). The universe of discourse for (e, \dot{e}) is taken within $(-1,1)$ and the output universe of discourse within the range $(0,1)$. Since, the valve takes positive values of voltage as input. The rules are listed in Table (7) and were selected by several trials to reach the best response. Also, the values of gains (k_p, k_v , and k_o) are tuned manually by several trials to achieve the desired specifications such as minimum overshoot, minimum oscillation and disturbance rejection, see Table (8).

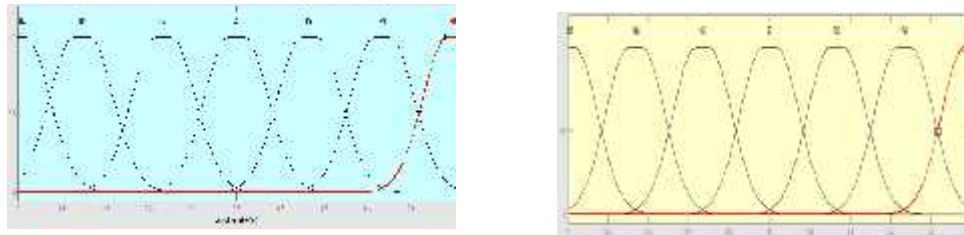


Figure (5): Inputs and output Membership functions.

A medical trajectory for the lower limb rehabilitation robot is selected as sinusoidal signal with frequency equal one Hz where this value approximately smeller to frequency of human during walking. This trajectory represents the left and right rotation for the first DOF, and flexion and extension for other DOFs. Figure (6) shows the block diagram of the closed loop controlled system of 4-DOF robot actuated by PMA and controlled by PD-FLC. Moreover, Figure (7) shows the Simulink of closed loop system.

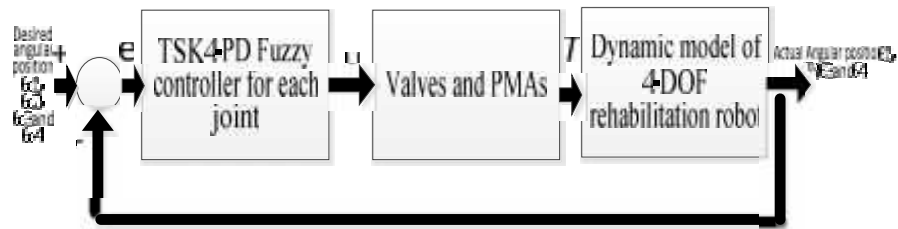


Figure (6): Block Diagram for closed loop system.

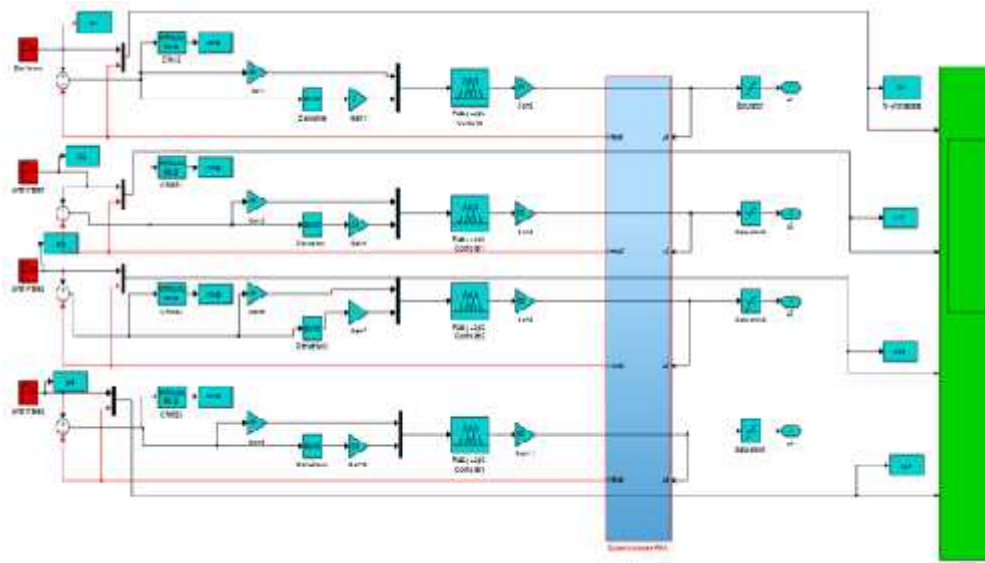


Figure (7): Simulink of the closed loop lower limb rehabilitation robot (4-DOF).

The Simulink block of the dynamic model is shown in Figure (8), equations (1 to 7), and the Simulink of the valves and PMAs is shown in Figure (9), equations (11 to 13). Moreover, the Simulink of the joint friction model is shown in Figure (10), equations (8 to 10). Also, the model of friction of PMA is shown in figure (11), equations (14 and 15).

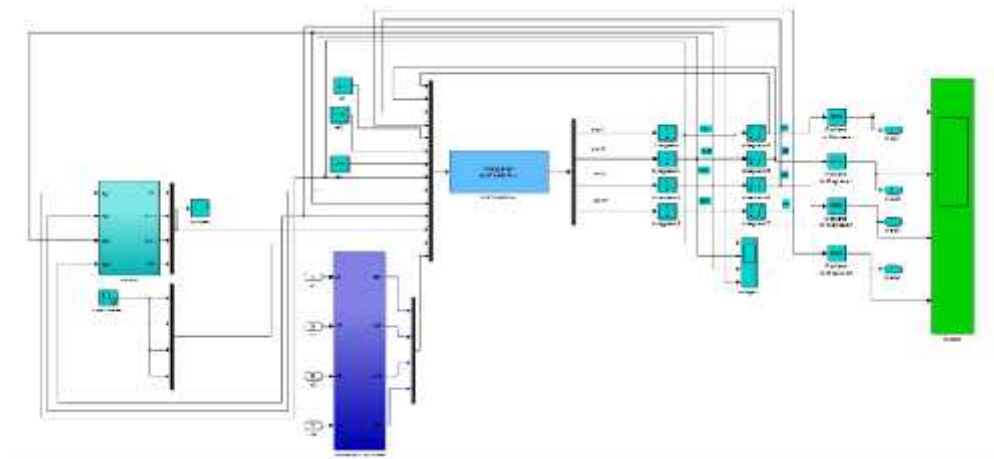


Figure (8): Simulink of the dynamic model of the robot (4-DOF) robot with friction and disturbance.

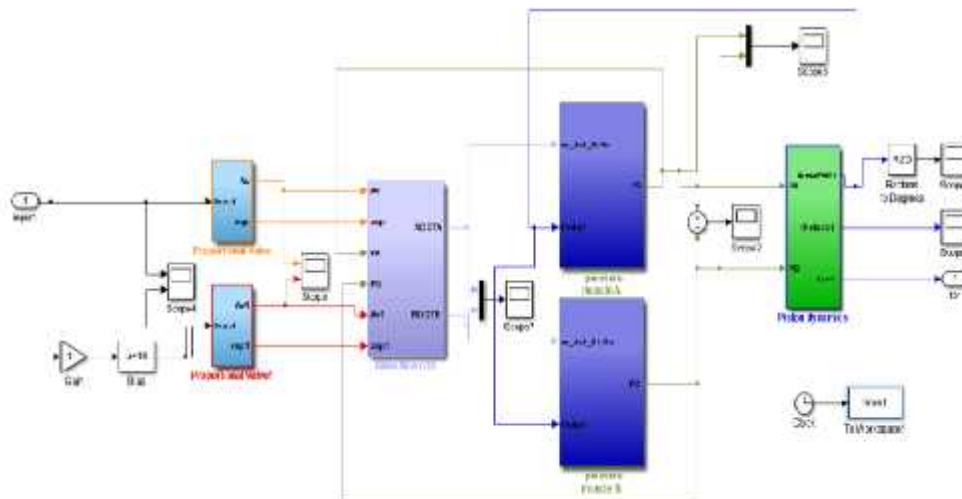


Figure (9): Simulink for PMAs and valves.

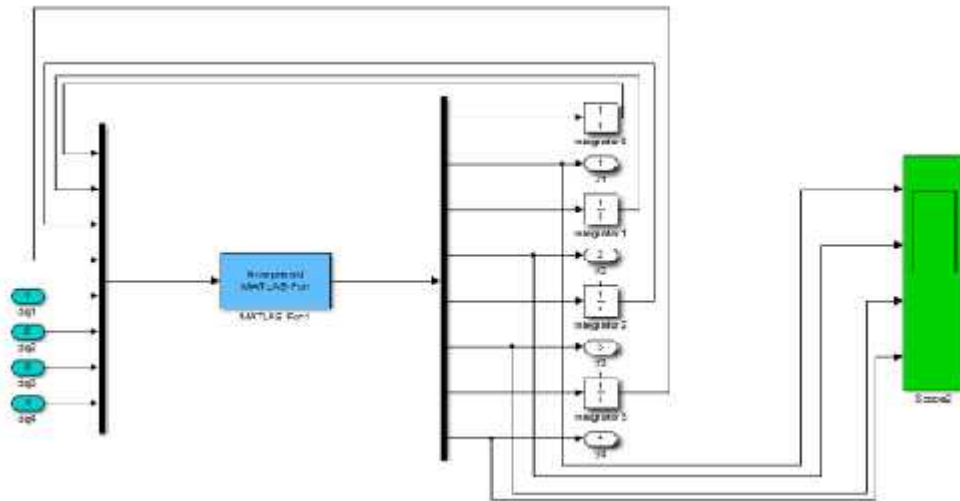


Figure (10): Model of joint friction.

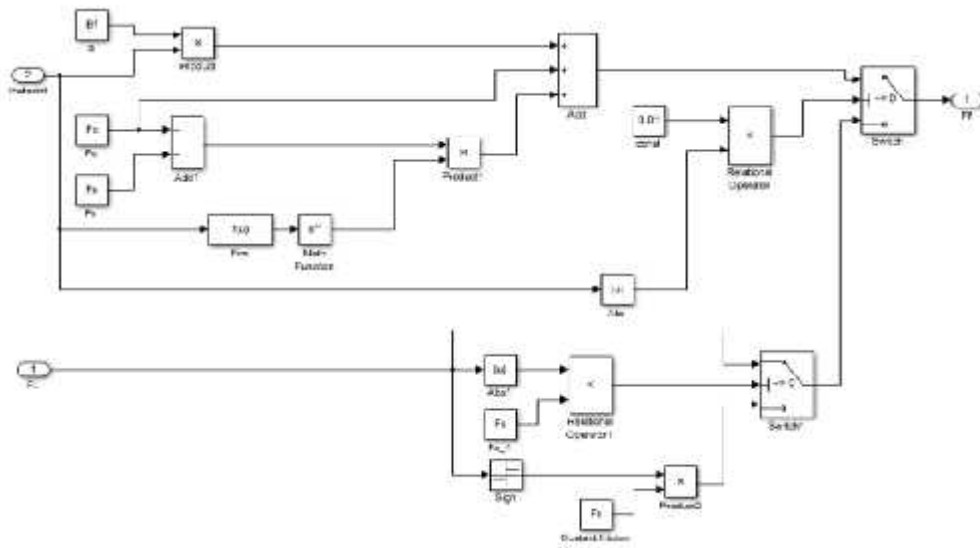
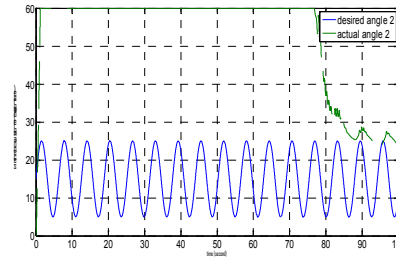
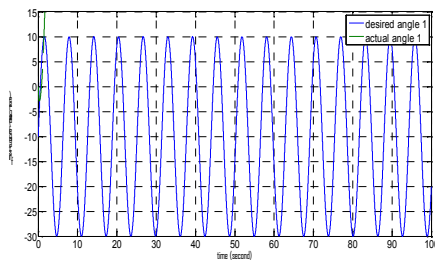
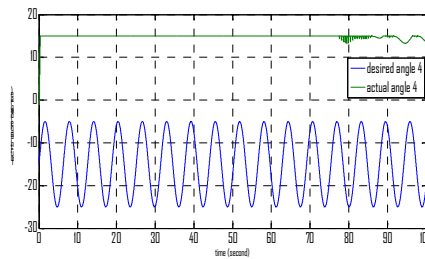
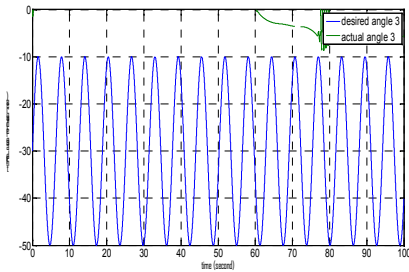


Figure (11): PMA friction model.

By applying the reference trajectory on the joints of the robot, the joints angle responses are shown in Figure (12). It can be motive from the results that the friction, disturbance and the nonlinearity of the dynamic model have a strong and negative influence on the response of robot joints. So, the Mamdani fuzzy control algorithms cannot guarantee the needed control precision. In order to cope with these influences, a FLC TSK type is used. Using the same specifications of the Membership type for the inputs and select the output Membership functions of the output as seven linear ones, Figure (13) shows the response of the closed loop controlled system using TSK PD-like fuzzy controller.

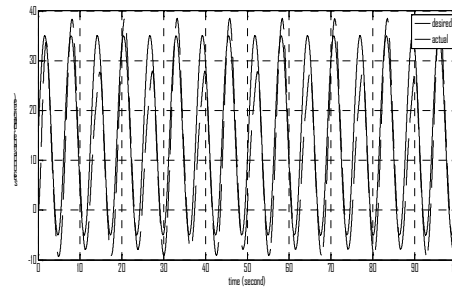
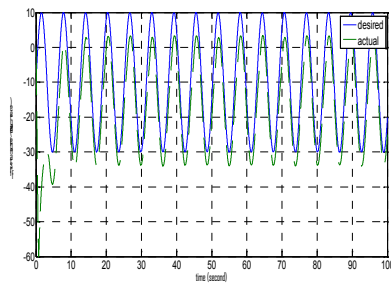


(a): Hip internal/ external rotation angle. (b): Hip flexion/ extension angle.

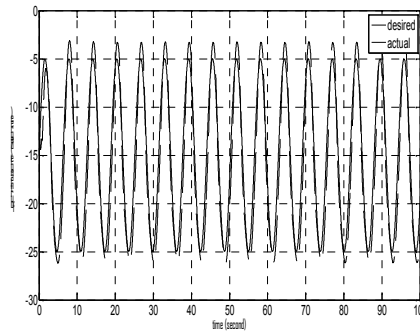
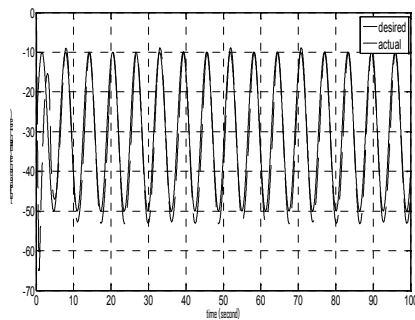


(c): Knee flexion/extension angle. (d): Ankle flexion/ extension angle.

Figure (12): Closed loop joints angles response using Mamdani PD-fuzzy controller.



(a): Hip internal/ external rotation (b): Hip flexion/ extension angle.



(c): Knee flexion/extension angle. (d):Ankle flexion/ extension angle.

Figure (13): Closed loop joints angles response using TSK-PD-fuzzy controller.

6. Conclusions:

In this work, 4-DOF lower limb rehabilitation robot was designed and simulated. It was actuated by using PMAs and the effects of frictions and disturbances were taken into consideration. The singularity problem of inertia matrix was solved by adding a fixed link to the structure. Position controllers incorporate Mamdani type and TSK type PD-like fuzzy logic position controllers were used to control the robot. A comparison between the results of the Mamdani type and (TSK) type shows the superiority the TSK-PD-like fuzzy controller to satisfy the desired requirements such as minimum overshoot, minimization of oscillation and disturbance rejection as with using Mamdani type. The percentages of enhancement for the oscillation error in the position are 66%, 92%, 81% and 93% for each DOF respectively.

7. References:

- {1}. T. Nef, M. Mihelj and R. Riener, "ARMin: a robot for patient-cooperative armtherapy", *Medical and Biological Engineering and Computing*, Vol. 45, PP. 887-900, 2007.
- {2}. I. P. Herman, *physics of human body*, springer, 2007.
- {3}. G. A. Ollinger, J. E. Colgate, M. A. Peshkin and A. Goswami, "Active-Impedance Control of a Lower-Limb Assistive Exoskeleton", *Proceedings of the 2007 IEEE 10th International Conference on Rehabilitation Robotics*, June 12-15, Noordwijk, Netherlands, PP. 188-195, 2007.
- {4}. G. A. Ollinger, J. E. Colgate, M. A. Peshkin and A. Goswami, "Design of an Active 1-DOF Lower-Limb Exoskeleton with Inertia Compensation", *IEEE*, Sept 2, 2010.
- {5}. T. D. Thanh, and T. ThienPhuc, "Neural Network Control of Pneumatic Artificial Muscle Manipulator for Knee Rehabilitation", *Science & Technology Development*, Vol 11, No.03, 2008.
- {6}. E. Akdoğan and Z. Şişman, "A Muscular Activation Controlled Rehabilitation Robot System", A. König et al. (Eds.): *KES 2011, Part I*, LNAI 6881, pp. 271–279, Springer-Verlag Berlin Heidelberg, 2011
- {7}. W. Aminiazar, F. Najafi and M. A. Nekoui, "Optimized intelligent control of a 2-degree of freedom robot for rehabilitation of lower limbs using neural network and genetic algorithm", *Journal of Neuro Engineering and Rehabilitation*, Vol. 10, No. 96, 2013.
- {8}. M. W. Spong, S. Hutchinson and M. Vidyasagar, *Robot Modelling and Control*, John Wiley& Sons Inc, Edition, USA, 2005.
- {9}. E. Kelasidi¹, G. Andrikopoulos, G. Nikolakopoulos and S. Manesis, "A Survey on Pneumatic Muscle Actuators Modeling", *Journal of Energy and Power Engineering* Vol. 6, PP. 1442-1452, 2012.
- {10}. T. Driver, "Innovation For Powered Prostheses Utilizing Pneumatic Actuators", PhD Dissertation, The University of Alabama, 2012.
- {11}. G. Kothapalli and M. Y. Hassan, "Design of a Neural Network Based Intelligent PI Controller for a Pneumatic System", *IAENG International Journal of Computer Science*, Vol.35, No. 2, 2008.
- {12}. K. Junius, "Design of an Actuated Orthosis for Support of the Sound Leg of Transfemoraldysvascular Amputees", M. Sc. thesis, Faculty of Engineering, Department of Mechanical Engineering, 2012.

{13}. Ž. Šitum, and S. Herceg," Design and Control of a Manipulator Arm Driven by Pneumatic Muscle Actuators", 16th Mediterranean Conference on Control and Automation Congress Centre, Ajaccio, France June 25-27, 2008.

Appendix

Table (1): DH Parameters

Joint	Movement	θ	α	d	a
Hip	I/E Rotation	0	0	0	0
Hip	F/E	-90	0	0	0
Knee	F/E	0	0	0	0
Ankle	F/E	0	0	0	0

Table (2): ROM of joint angles of proposed robot.

DOF	ROM
I/E rotation (Hip)	+15° to -60°
F/E (Hip)	+60° to -15°
F/E (knee)	0° to -65°
F/E (ankle)	+15° to -35°

Table (3): The values of peak torque {13}.

Joint / segment movement	Biol.ROM (max)	Peak torque
Hip / internal/external rotation	+15° to -60°	60 N/m
Hip flexion/extension	+140° to -15°	65 N/m
Knee flexion/extension	0° to -140°	60 N/m
Ankle flexion/extension	+20° to -50°	60 N/m

Table(4): Parameters of the valve and PMA {10}, {11}.

Parameters of actuator system	Value
Valve constant	$C_v = 3.15745$ $10^{-4} m^3/V$
Maximum effective area of valve	$C_v = 3.1574/V$ $+ 10^{-4} 16.28$ $A_{vmax} = m^2$ 10^{-6}
Valve coefficient of discharge	$A_{vm} = 294$ $C_f = C$
ratio of specific heats	$\gamma = 1.4$
the gas temperature,	$T = 293$ K
critical pressure ratio	$\beta_c = 0.528$
Supply pressure	$P_s = 405$ KPa
the atmospheric pressure	$P_a = 10$ KPa
fixed muscle thread length	$b = 0.7$ m
the number of turns of the braided threads	$n = 2.4$
The initial length of the muscles	$l_0 = 0.5$ m
the moment of inertia	$I = 0.154$ Kgm^2
the damping coefficient	$B = 0.01$ $Kgm^{-1}s$
the stiffness coefficient	$E = 20.748$ $KKgm^2/s^2$

Table (5): Joint Friction Parameters {7}

Friction parameter	Value	Friction parameter	value
Stiffness coefficient	0.1 Nms/rad	Coulomb friction	1 Nm
Damping coefficient	50 Nms/rad	Coulombic friction	1.5 Nm
Coefficient of viscous friction	0.4 Nms/rad	Stribeck velocity	1 rad/sec

Table (6): PMA friction parameter {11}.

Friction parameter	Value
Stribeck exponent	$n = 2;$
Coulomb friction	$F_c = 24 \text{ Nm}$
Viscous friction coefficient Nm	$F_v = 24 \text{ Nm}$
External Load acting on the piston	$FL = 8 \text{ N}$
Static friction	$F_s = 65 \text{ N}$
Stribeck speed rad/sec	$v_s = 4 \text{ rad/sec}$

Table (7): Rules of PD-like position FLC.

	NB	NM	NS	Z	PS	PM	PB
NB	NB	NB	NB	NB	NM	NS	Z
NM	NB	NB	NB	NM	NS	Z	PS
NS	NB	NB	NM	NS	Z	PS	PM
Z	NB	NM	NS	Z	PS	PM	PB
PS	NM	NS	Z	PS	PM	PB	PB
PM	NS	Z	PS	PM	PB	PB	PB
PB	Z	PS	PM	PB	PB	PB	PB

Table (8): gains of the PD-like FLC

Gain	Value
Kp1	0.049
Kv1	0.2
Ko1	10
Kp2	0.033
Kv2	0.04
Ko2	10
Kp3	0.044
Kv3	0.1
Ko3	10
Kp4	0.066
Kv4	0.04
Ko4	10

نمذجة وتصميم مسيطر مسار لروبوت إعادة تأهيل الأطراف البشرية السفلية باستعمال مشغل العضلة الهوائية

أ.م.د. محمد يوسف حسن* شهد صبيح غنتاب**

المستخلص

الهدف من روبوتات إعادة التأهيل الخاصة بالأجزاء السفلية للأطراف البشرية هو إعادة القدرة على المشي وتقوية العضلات. يقدم البحث نمذجة وتصميم لروبوت مكون من أربع درجات من الحرية، اثنين منها في مفصل الورك، وواحدة في مفصل الركبة والرابعة في مفصل الكاحل، يتم تحريك المفاصل باستعمال مشغلات العضلة الهوائية، إذ أن هذا النوع من المشغلات يعد الأفضل في التطبيقات الطبية؛ نظراً لخواصه المشابهة للعضلات البشرية. يحل البحث مشكلة تمييز نهاية المحور بالنسبة لقاعدة محاور الروبوت عن طريق إضافة إزاحة. ويأخذ البحث بنظر الاعتبار الاحتكاك في المفاصل والمحركات جميعها، والاضطرابات الخارجية المؤثرة في المفاصل. إذ إن الروبوت المقترح للساق الأيمن، يمكن استعماله من قبل الأشخاص فوق سن 40 سنة، وقد تم اعتماد أطوال وأوزان هذه الفئة العمرية في أثناء التصميم. وعلى الرغم من اللاخطية العالية في التصميم، إلا أنه تمت السيطرة على تتبع المسارات الطبية عن طريق مسيطر منطق ضبابي ذكي متناسب. متفاضل ومقارنة بين نوعين منه Mamdani و TSK. وذلك لغرض تحقيق المواصفات المطلوبة مثل تقليل تجاوز المدخل وتقليل التذبذب و مقاومة الاضطرابات حيث أثبتت النتائج ان TSK نتائجه أفضل من النوع الثاني.

الكلمات المفتاحية: مسيطر الموضع, روبوت إعادة تأهيل الأطراف البشرية, مشغلات العضلة الهوائية, والمسيطر الضبابي.